Tracer diffusion in a random barrier model: The crossover from static to dynamic disorder

Andrey Milchev,[1] Jordan Brankov,[2] and Victor D. Pereyra[3,*]
[1]Institute for Physical Chemistry, Bulgarian Academy of Sciences, 1113 Sofia, Bulgaria
[2]Institute for Mechanics, Bulgarian Academy of Sciences, 1113 Sofia, Bulgaria
[3]Departamento Fisica and Centro Latinoamericano de Estudios Ilya Prigogine, Universidad Nacional de San Luis, CONICET, Chacabuco y Pedernera, 5700 San Luis, Argentina

(Received 11 September 1997; revised manuscript received 2 June 1998)

In earlier investigations, we have shown that in a frozen-in random barrier environment the diffusive behavior of a thermally activated tracer particle shows a crossover from anomalous to normal diffusion, governed by the percolation threshold of the underlying lattice and the degree of randomness of these barriers. Changes due to a periodic renewal of the environment were not considered. In the present work, we use an analysis within the framework of the effective medium approximation, and Monte Carlo simulations, to study the crossover from a ''frozen in'' static to *dynamically* updated random barrier disorder with changing temperature T, and find a temperature transition to a qualitatively different type of diffusive behavior of the tracer particle. It turns out that the Arrhenius relationship of diffusion coefficient D on T is replaced by a linear one at a crossover temperature T_c, which itself depends on the frequency of environmental renewal ω with a power law: $T_c \propto \omega^{\delta}$, with $\delta = 0.21 \pm 0.02$. In the linear regime below T_c, where we find that the tracer movement is highly correlated, the average effective activation energy for diffusion $\langle E_a \rangle$ is equal to the thermal energy of the tracer, $\langle E_a \rangle \approx kT$, while for $T > T_c$ (Arrhenian regime) the random walks are practically uncorrelated and $\langle E_a \rangle$ is constant, given by the mean value of the barrier heights probability distribution, $\overline{E}$. These results are found to be independent of the particular type of probability distribution which is used for the barrier heights. [S1063-651X(98)07310-3]

PACS number(s): 05.40.+j, 05.60.+w

I. INTRODUCTION

Recently in a series of papers [1–4] we studied the diffusion in the presence of randomly distributed static barriers by means of Monte Carlo (MC) computer simulations. A characteristic change in behavior from anomalous diffusion with mean square displacement (MSQD) $\langle R(t)^2 \rangle \propto t^{\gamma}$, with $\gamma < 1$, to normal diffusion $\langle R(t)^2 \rangle \propto t$, was found to occur at crossover time $\tau_c \propto \exp(E_{\rm eff}/kT)$, where the effective activation energy $E_{\rm eff}$ was shown to be determined by the percolation threshold of the underlying lattice and the dispersion in the probability distribution function (PDF) of the barriers. An interesting feature in the temperature behavior of the diffusion coefficient D in disordered lattices is the observed *Arrhenian* dependence on inverse temperature which reflects the compensation of opposite curvature [5] for the cases of random traps and barriers when these two types of disorder are both present in amorphous solids. A special example of a purely Arrhenian D vs T relationship constitutes the square lattice [3,6], where self-duality and symmetric probability densities [7] lead to an effective insensitivity with respect to barrier disorder. For different PDF's of the barriers and lattice geometry, deviations from Arrhenian behavior are clearly manifested [3,6]. In the presense of an external field is has recently been shown [4,8] that increasing temperature may even systematically *reduce* the MSQD $\langle R(t)^2 \rangle$ in the random barrier model (RBM).

In all studies quoted above, the random medium has been assumed to be frozen, i.e., as a static distribution of random barriers over the lattice. In reality, however, the random environment may itself be periodically updated while the walker proceeds in the host matrix.

Indeed, as suggested in Ref. [9], one may identify self-diffusion in liquids with the case of dynamic disorder when the mean time for the system evolution renewal $\tau_{\rm ren}$ is comparable with the average particle hopping time $\tau_{\rm hop}$. In cases when $\tau_{\rm ren} \gg \tau_{\rm hop}$, that is, in cases of static disorder, one deals with a situation when a description in terms of conventional percolation theory should be appropriate [1]. In contrast, for $\tau_{\rm ren} \approx \tau_{\rm hop}$ the tracer cannot explore the energetic landscape ''easy'' paths, since low barriers are constantly created and most of the jumps are successful. This problem has been treated theoretically in a series of works [9–11] which showed that if the concurrent motion of the host is modeled by random reassignment of hopping probabilities with a constant probability ω per unit time for renewal to occur, the frequency-dependent diffusion coefficient $D(\Omega)$ with renewal is obtainable from $D(\Omega)$ without renewal through the formal substitution $i\Omega \rightarrow i\Omega + \omega$. In this way, an expression for the MSQD with renewal in terms of the MSQD without renewal can also be derived. Very few models for diffusion with disorder, however, may be solved analytically, even within the framework of the widely used effective medium approximation (EMA) [12–15], down to closed expressions for $D(\Omega)$ without renewal. Therefore, computer simulations suggest an efficient approach to learn more about diffusion with dynamic disorder, and are the main tool used in the present investigation.

A gradual transition from static to dynamic disorder can

*Author to whom correspondence should be addressed. Electronic address: vpereyra@unsl.edu.ar

be accomplished if the barriers are updated periodically with some frequency ω, and the temperature variation of D is studied at each ω within a broad interval. This is in fact the main objective of the present work. At any $\omega \neq 0$ we find clear evidence for two regimes of diffusive behavior: a high-temperature (nearly Arrhenian) one, and a low-temperature regime, in which the diffusion coefficient is linearly proportional to the thermal energy kT. Our simulational results show that this finding holds independently of the particular probability distribution in the RBM, provided barriers of zero height may also occur.

In Sec. II we recall the main premises of the model and its treatment within the framework of the EMA (Sec. III), demonstrating some important limiting cases where simple analytical expressions expose the main physics of the expected diffusive behavior. The crossover to non-Arrhenian diffusive behavior at low temperature is shown by solving numerically the characteristic self-consistency equation of the EMA for the case of a square lattice. For hops and simultaneous $\omega = 1$ environment renewal, a very simple analytical expression is shown to yield perfect agreement with our computer experiment. In Sec. IV we report our main MC results for two different PDF's of energy barriers, and demonstrate their good agreement with EMA results, irrespective of the particular PDF being used. Eventually, in Sec. V we summarize our observations.

II. MODEL

In the present investigation, as before, the random barriers define transition rates which are governed by Boltzmann statistics in a standard fashion. Only jumps between adjacent sites are allowed, and the barrier energies (saddle points) are assigned values E_{ij} at random subject to a specific probability distribution function. The transition rates Γ_{ij} from site i to site j are given by the Arrhenius law

$$\Gamma_{ij} = \Gamma_0 \frac{1}{z} \exp(-E_{ij}/kT), \tag{1}$$

where z denotes the coordination number of the lattice. If the transition rates are converted into probabilities by dividing them by Γ_0, the difference of the sum over all neighbor sites from 1 gives the probability for the particle to make no jump whatsoever and remain on spot:

$$\frac{\Gamma_{ii}}{\Gamma_0} = 1 - \sum_{j\ (\neq i)} \frac{\Gamma_{ij}}{\Gamma_0}. \tag{2}$$

As long as the barriers are not updated, once a forward jump is made in a particular direction the backward jump (back to the original position) should carry the same probability as the forward jump. Within the RBM the barrier heights are distributed at random subject to a probability function which may represent either a uniform distribution

$$\nu(E) = \begin{cases} \dfrac{1}{2\sigma E_0} & (1-\sigma)E_0 \leq E \leq (1+\sigma)E_0 \\ 0 & \text{otherwise}, \end{cases} \tag{3}$$

where E is a random number between 0 and 1, the dispersion parameter σ ranges in the interval 0 and 1 so as to control the width of the distribution, or an exponential PDF:

$$\nu(E) = \frac{1}{E_0} \exp\left(-\frac{E}{E_0}\right), \tag{4}$$

where there is no additional dispersion parameter. The mean barrier energy is always kept constant at the value $E_0 = 0.5$.

III. EMA ANALYSIS

The EMA for hopping transport of particles was developed by Summerfield [12], Odagaki and Lax [13], and Webman [14]; for a review, see Ref. [15]. The scheme followed by the EMA is the following: One starts with the master equation for the probability $P(\mathbf{r}_i, t)$ of finding a particle at site $\mathbf{r}_i$ at time t,

$$\frac{d}{dt} P(\mathbf{r}_i, t) = \sum_{j \neq i} [\Gamma_{ji} P(\mathbf{r}_j, t) - \Gamma_{ij} P(\mathbf{r}_i, t)]. \tag{5}$$

In the effective medium approximation, the set of static jump frequences Γ_{ij} is replaced by a single, position-independent, but frequency-dependent, effective jump frequency, $\tilde{\Gamma}$ [2]. The Laplace-transformed master equation then reads

$$s\tilde{P}(\mathbf{r}_i, s) - \delta_{i,0} = \tilde{\Gamma}(s) \sum_{j \neq i} [\langle \tilde{P}(\mathbf{r}_j, s) \rangle - \langle \tilde{P}(\mathbf{r}_i, s) \rangle]. \tag{6}$$

From the solution of this equation, the Laplace transform MSQD is obtained as

$$\langle \tilde{r}^2(s) \rangle = z a^2 \tilde{\Gamma}(s)/s^2, \tag{7}$$

whereby a denotes the lattice constant, and cubic lattices are assumed. If the effective transition rate approaches a constant value in the limit $s \to 0$, the resulting MSQD is linear in time for large times,

$$\langle r^2(t) \rangle \to_{t\to\infty} z a^2 \tilde{\Gamma}(s \to 0) t, \tag{8}$$

and the asymptotic diffusion coefficient is given by $D = \tilde{\Gamma}(s \to 0)$.

The effective jump frequency $\tilde{\Gamma}$ has to be determined from a *self-consistency* condition, which within the so-called *single-bond* EMA is given by, e.g. [15],

$$\left\langle \frac{\Gamma - \tilde{\Gamma}(s)}{1 + 2[\Gamma - \tilde{\Gamma}(s)][1 - s\tilde{P}^M(\mathbf{0}, s)]/[z\tilde{\Gamma}(s)]} \right\rangle = 0. \tag{9}$$

Here $\langle\ \rangle$ denotes averaging over the probability distribution of Γ, the random jump rate of a selected lattice bond; and

$$\tilde{P}^M(\mathbf{0},s)=\frac{1}{(2\pi)^d}\int_{-\pi}^{\pi}\cdots\int_{-\pi}^{\pi}d^dk\frac{1}{s+z\tilde{\Gamma}(s)[1-p(\mathbf{k})]} \tag{10}$$

is the Laplace transform of the initial site occupation probability, where $p(\mathbf{k})$ is the structure function. For nearest-neighbor transitions on d-dimensional simple cubic lattices with a unit lattice constant, the structure function is given by

$$p(\mathbf{k})=\frac{1}{d}\sum_{i=1}^{d}\cos k_i\,. \tag{11}$$

We shall use the fact that $\tilde{P}^M(\mathbf{0},s)$ is simply related to the lattice Green function $P(\mathbf{n},\xi)$,

$$P(\mathbf{n},\xi)=\frac{1}{(2\pi)^d}\int_{-\pi}^{\pi}\cdots\int_{-\pi}^{\pi}\mathrm{d}^dk\frac{\cos(\mathbf{n}\cdot\mathbf{k})}{1-\xi p(\mathbf{k})}, \tag{12}$$

by the equation

$$\tilde{P}^M(\mathbf{0},s)=\frac{1}{s+z\tilde{\Gamma}(s)}P[\mathbf{0},\xi(s)], \tag{13}$$

where

$$\xi(s)=\left[1+\frac{s}{z\tilde{\Gamma}(s)}\right]^{-1}. \tag{14}$$

In order to carry out the averaging over the distribution of jump rates in the self-consistency equation [Eq. (9)], one first determines the rate density $\rho(\Gamma)$ by the transformation

$$\rho(\Gamma)=\nu[E(\Gamma)]\left|\frac{dE}{d\Gamma}\right|. \tag{15}$$

For the case of a uniform PDF of barrier heights, one obtains, from Eqs. (1), (3), and (15),

$$\rho(\Gamma)=\begin{cases}\dfrac{kT}{2\sigma E_0}\dfrac{1}{\Gamma} & \text{if } \Gamma_{\min}\leqslant\Gamma\leqslant\Gamma_{\max}\\ 0 & \text{otherwise,}\end{cases} \tag{16}$$

where, from Eq. (2),

$$\Gamma_{\min}=\Gamma_0\exp\left[-\frac{(1+\sigma)E_0}{kT}\right],\quad \Gamma_{\max}=\Gamma_0\exp\left[-\frac{(1-\sigma)E_0}{kT}\right]. \tag{17}$$

By performing the averaging in Eq. (9) with the probability density (16), one obtains the following explicit form of the EMA equation:

$$\ln\frac{1+g(s)[\Gamma_{\max}-\tilde{\Gamma}(s)]}{1+g(s)[\Gamma_{\min}-\tilde{\Gamma}(s)]}=g(s)\tilde{\Gamma}(s)\ln\frac{\Gamma_{\max}}{\Gamma_{\min}}, \tag{18}$$

where

$$g(s)=\frac{2}{z\tilde{\Gamma}(s)}[1-s\tilde{P}^M(\mathbf{0},s)]. \tag{19}$$

Next, by making use of definitions (17), and introducing the reduced mean barrier energy ϵ_0,

$$\epsilon_0=E_0/kT,\quad \bar{\Gamma}=\Gamma_0\exp(-\epsilon_0), \tag{20}$$

we rewrite Eq. (18) in a form more convenient for analysis:

$$\frac{\tilde{\Gamma}(s)}{\bar{\Gamma}}=\frac{\sinh\{\sigma\epsilon_0[1-\phi(\xi)]\}}{\sinh[\sigma\epsilon_0\phi(\xi)]}\,\frac{\phi(\xi)}{[1-\phi(\xi)]}. \tag{21}$$

Here $\xi=\xi(s)$ is defined in Eq. (14), and

$$\phi(\xi(s))\equiv g(s)\tilde{\Gamma}(s)\equiv\frac{2}{z}\{1-[1-\xi(s)]P(\mathbf{0},\xi(s))\}. \tag{22}$$

Note that in the one-dimensional case the above expressions significantly simplify, since then

$$P(\mathbf{0},\xi)=\sqrt{1-\xi^2},\quad d=1 \tag{23}$$

and

$$\phi(\xi(s))=1-\sqrt{\frac{1-\xi(s)}{1+\xi(s)}}=1-\sqrt{\frac{s}{s+4\tilde{\Gamma}(s)}},\quad d=1. \tag{24}$$

A. Limit of vanishing disorder

From Eq. (21) it immediately follows that in the limit of vanishing disorder, $\sigma\to0$, which implies $x\equiv\sigma\epsilon_0\to0$, one obtains the solution for a regular lattice, $\tilde{\Gamma}(s)=\bar{\Gamma}$. The corrections are of the order $O(x^2)$, as follows by expanding the right-hand side of Eq. (21) in powers of x,

$$\frac{\tilde{\Gamma}(s)}{\bar{\Gamma}}=1+\frac{1}{6}x^2\phi(\xi)[1-2\phi(\xi)]+O(x^4), \tag{25}$$

setting

$$\tilde{\Gamma}(s)/\bar{\Gamma}=1+\beta^2\gamma_2(s)+O(\beta^4), \tag{26}$$

and expanding $\xi=\xi(s)$ given by Eq. (14) around

$$\xi_0(s)=\left[1+\frac{s}{z\bar{\Gamma}}\right]^{-1}. \tag{27}$$

The latter expansion yields, for $\phi(\xi(s))$ [see Eq. (22)]

$$\phi(\xi(s))=\frac{2}{z}\{1-[1-\xi_0(s)]P(\mathbf{0},\xi_0(s))\}+O(x^2). \tag{28}$$

Thus, for the correction term in Eq. (26), one obtains

$$\gamma_2(s) = \frac{4}{3z^2}\{1-[1-\xi_0(s)]P(\mathbf{0},\xi_0(s))\} \times \{[1-\xi_0(s)]P(\mathbf{0},\xi_0(s))-1+z/4\}. \quad (29)$$

Note that for any positive s from definition (27), it follows that $\xi_0(s)<1$, and one can make use of the analyticity of the lattice Green function $P(\mathbf{n},\xi)$ in the unit circle [15]. In particular, one has the convergent series expansion

$$P(\mathbf{0},\xi) = \sum_{n=0}^{\infty} P_n(\mathbf{0})\xi^n, \quad |\xi|<1. \quad (30)$$

Here

$$P_n(\mathbf{0}) = \frac{1}{(2\pi)^d}\int_{-\pi}^{\pi}\cdots\int_{-\pi}^{\pi} \mathrm{d}^d k[p(\mathbf{k})]^n \quad (31)$$

is the probability that a random walker on the regular lattice, starting at the origin, will return to the origin (not necessarily for the first time) after a walk of n steps.

If $s/\Gamma\to\infty$, then $\xi_0(s)\to 0$ and since for the simple-cubic lattices one has $P_{2k+1}(\mathbf{0})=0$, $k=0,1,2,\ldots$, Eq. (30) yields

$$P(\mathbf{0},\xi) = 1+P_2(\mathbf{0})\xi^2+O(\xi^4), \quad \xi\to 0. \quad (32)$$

Then expression (29) simplifies to

$$\gamma_2(s) = \tfrac{1}{3}\Gamma/s + O(\Gamma^2/s^2), \quad \Gamma/s\to 0 \quad (33)$$

for all dimensionalities d.

B. High-temperature limit

The high-temperature limit is almost identical to the vanishing disorder limit. Indeed, $\epsilon_0\to 0$ implies $x=\sigma\epsilon_0\to 0$, and expansions (25) and (26) hold true. The only difference is that now the expression for $\overline{\Gamma}$ [see Eq. (20)], has to be expanded in powers of ϵ_0. Obviously, this ammounts to expanding the $\overline{\Gamma}$-dependent quantity $\xi_0(s)$ around $\overline{\Gamma}=\Gamma_0$ in the final result Eq. (29) for $\gamma_2(s)$. In the leading order of magnitude one recovers the results given by Eqs. (29) and (33), with Γ replaced by Γ_0.

C. Small s limit (rare renewal)

When $s\to 0$, under the assumption that $s/\widetilde{\Gamma}(s)\to 0$ as well, Eq. (14) implies that $\xi(s)\to 1^-$. The lattice Green function $P(\mathbf{0},\xi)$ then has well known singularities, which strongly depend on the dimensionality d: it diverges like $(1-\xi)^{-1/2}$ for $d=1$, diverges logarithmically like $\ln(1-\xi)^{-1}$ for $d=2$, and approaches a finite value for all $d\geqslant 3$. In any case, as it can be seen from Eq. (22), $\phi(\xi(s))\to 2/z$ as $s\to 0$. Therefore, the limit $s\to 0$ on the right-hand side of Eq. (21) exists and, directly yields

$$\widetilde{\Gamma}(s=0) = \Gamma\frac{2}{z-2}\frac{\sinh[\sigma\epsilon_0(1-2/z)]}{\sinh(2\sigma\epsilon_0/z)}. \quad (34)$$

The above result coincides with Eq. (14) in Ref. [3].

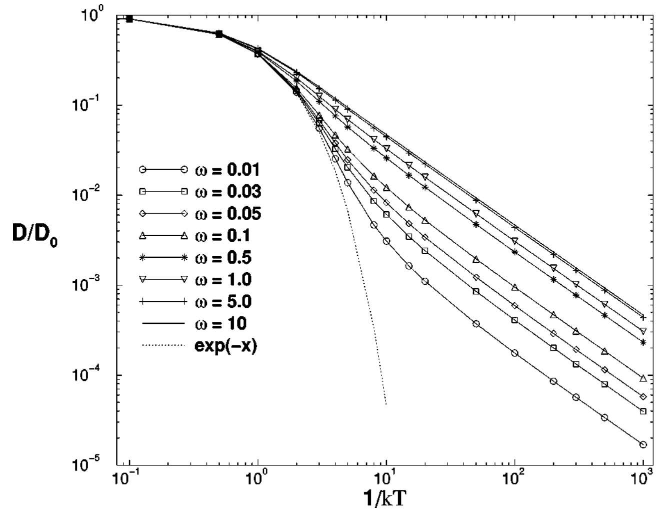

FIG. 1. Variation of the diffusion coefficient with inverse temperature for various update frequences ω derived from the EMA—Eq. (21) for the square lattice. A dotted line denotes a purely Arrhenian behavior.

D. Large s limit (frequent renewal)

As mentioned in Sec. I, the large s limit is involved in obtaining the diffusion coefficient in a dynamically disordered medium with extremely high renewal frequency ω. Assuming that $s/\widetilde{\Gamma}(s)\to\infty$, one obtains from Eq. (14) that $\xi(s)\to 0$. The latter implies the validity of expansion (32) for the lattice Green function. Then, from Eq. (22), it immediately follows that

$$\phi(\xi) = (2/z)\xi + O(\xi^2)\to 0, \quad \xi\to 0. \quad (35)$$

In the limit $\phi(\xi)\to 0$, the EMA equation (21) reduces to

$$\widetilde{\Gamma}(s)/\overline{\Gamma} \simeq \sinh(x)/x. \quad (36)$$

Hence, by taking into account that

$$\overline{\Gamma}\sinh(x) = (\Gamma_{\max}-\Gamma_{\min})/2, \quad (37)$$

we obtain from Eq. (36) the leading-order result

$$\widetilde{\Gamma}(s\to\infty) \simeq \frac{\Gamma_{\max}-\Gamma_{\min}}{2\sigma}\frac{kT}{E_0}. \quad (38)$$

Obviously, in the limit of vanishing disorder $\sigma\to 0$, Eq. (38) reproduces the result for a regular lattice, $\widetilde{\Gamma}(s\to\infty)\simeq\overline{\Gamma}$. In the high-temperature limit $kT/E_0\to\infty$, by taking into account Eq. (17), one obtains from Eq. (38) the expected result $\widetilde{\Gamma}(s\to\infty)\simeq\Gamma_0$.

It is instructive to study now the low-temperature limit of Eq. (38), when $kT/E_0\to 0$. The behavior of $\widetilde{\Gamma}(s\to\infty)$ is nearly an Arrhenian one, dominated by the exponentially fast decay of $\Gamma_{\max}$, provided $\sigma<1$. However, in the case $\sigma=1$, which is our main concern here, and which corresponds to energy-barrier distribution starting from zero values, one obtains from Eq. (17) that $\Gamma_{\max}=\Gamma_0$ and $\Gamma_{\min}=\Gamma_0\exp(-2\epsilon_0)$. Then the following non-Arrhenian behavior takes place

$$\tilde{\Gamma}(s\to\infty)\simeq\Gamma_0\frac{kT}{2\sigma E_0},\quad kT/E_0\to 0. \tag{39}$$

This change from Arrhenian to power law (linear) dependence of the diffusion coefficient on temperature at small T is demonstrated on Fig. 1 for a square lattice, where Eq. (21) may be easily solved numerically (see the Appendix).

Evidently, the crossover from Arrhenian behavior to this low-temperature regime of diffusion occurs at temperatures which decrease as the renewal frequency is lowered. The variation of the crossover temperature, T_c, derived from Fig. 1, is shown below along with simulational data.

IV. SIMULATIONAL RESULTS

The MC simulation of the model is carried out in the usual way [1]. The particle is placed at time $t=0$ in the middle of the lattice, and a jump is attempted in a randomly chosen direction, whereby the corresponding barrier is assigned a value subject to Eqs. (3) and (4), and within the framework of a standard Metropolis procedure the probability to overcome the barrier [Eq. (1)] is compared to a random number in order to determine whether the attempt has been successful or not. Each attempt is considered a Monte Carlo step (MCS), and time is measured in MCS's. All barriers are updated at intervals of ω^{-1} MCS's, thus defining a frequency ω with which a renewal of the barrier landscape on the lattice is carried out. During the simulation a number of quantities are recorded, such as the mean square displacement $\langle R^2(t)\rangle$ of the tracer from which the diffusion coefficient D was determined; the correlation factor of the walks, f,

$$f=\lim_{N\to\infty}\frac{\langle R^2(N)\rangle}{N}, \tag{40}$$

where N is the number of steps; the average activation energy $\langle E_a\rangle$, etc.

In Fig. 2 we plot the variation of the dimensionless diffusion coefficient D/D_0 with inverse temperature for a number of update frequencies ω^{-1}. D_0 corresponds to $kT=\infty$ when the energy landscape surrounding a tracer is effectively smooth due to its own high thermal energy. Evidently, for quite different probability distributions of the barrier heights one observes the same crossover from Arrhenian dependence to a linear dependence of D/D_0 on kT at sufficiently low temperatures. From Fig. 2 one can see that the only difference between the uniform PDF, cf. Fig. 2(a), and the exponential PDF [Fig. 2(b)], comes from the essentially higher crossover temperature in the case of the exponential PDF (note that the average height of the barriers, $E_0=0.5$, is the *same* in both cases). This crossover depends on the frequency of environmental renewal ω. Evidently, with growing ω it occurs at higher and higher temperature T_c. For $\omega=0$ (static disorder) the crossover is then expected to take place at $T_c=0$, and one observes the familiar purely Arrhenian relationship $D/D_0\propto\exp(1/kT)$. It is also clear from Fig. 2 that the mobility of the tracer grows with increasing frequency ω. Thus we can distinguish between a high-temperature $T>T_c$ (Arrhenian) and a low-temperature $T<T_c$ regime for which $D/D_0\propto kT$, T_c depending on the frequency with which the random barriers are updated.

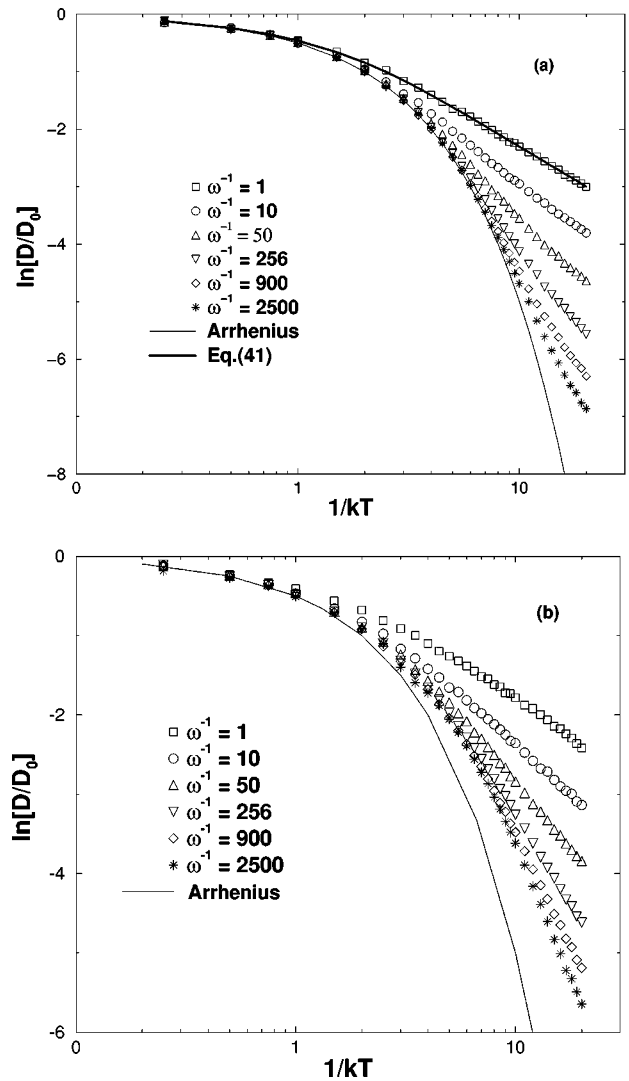

FIG. 2. Log-log plot of the reduced diffusion coefficient D/D_0 vs inverse temperature at different frequencies ω of the random environment renewal: (a) for the uniform PDF, and according to Eq. (41)—thick line. (b) For exponential PDF and Eq. (43) (thick full line). The solid line denotes a possible Arrhenian behavior.

This finding is in perfect quantitative agreement with the prediction of a simple result which can be derived analytically. In the case of complete renewal ($\omega=1$) the random walk of the tracer is entirely uncorrelated, and the diffusion coefficient is given by the averaged transition rate

$$D/D_0=\int_0^{E_{\max}}P(E)\exp(-\beta E)dE, \tag{41}$$

which for the uniform PDF yields

$$D/D_0=\frac{kT}{2E_0}\left[1-\exp\left(-\frac{2E_0}{kT}\right)\right]. \tag{42}$$

while for exponential PDF we have

$$D/D_0=\frac{kT}{(E_0+kT)}. \tag{43}$$

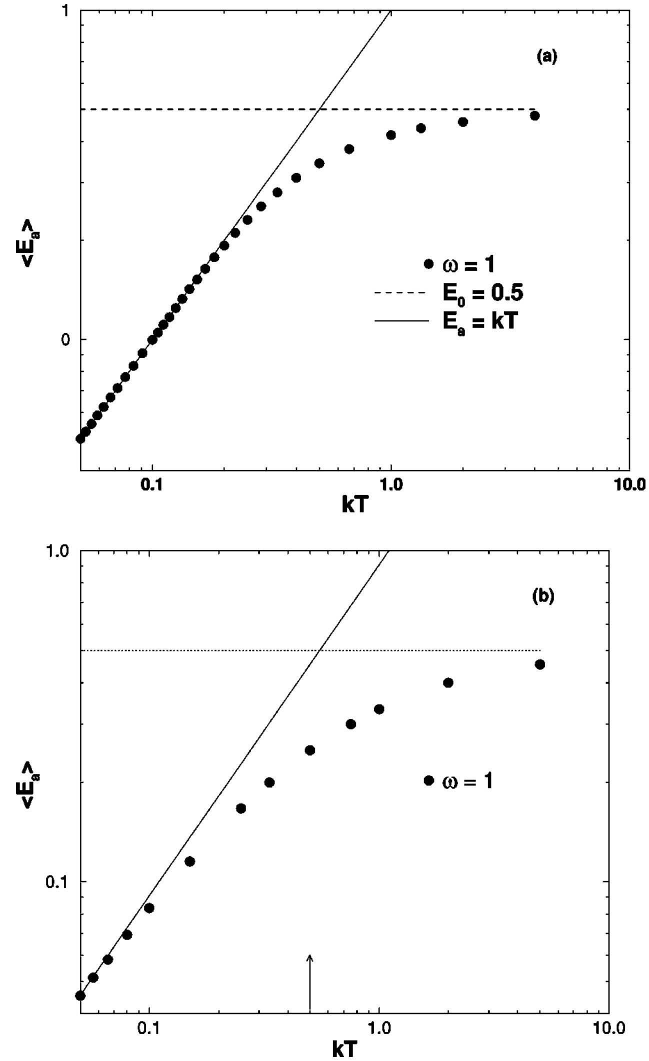

FIG. 3. Dependence of the measured average activation energy $\langle E_a \rangle$ on temperature for $\omega = 1$: (a) for the uniform PDF; (b) for the exponential PDF. Solid straight lines correspond to $\langle E_a \rangle \approx kT$, whereas dotted horizontal lines denote the mean value of the respective PDF's for the barrier heights. Arrows point to the respective intersection points of the straight lines at $kT = 0.5$.

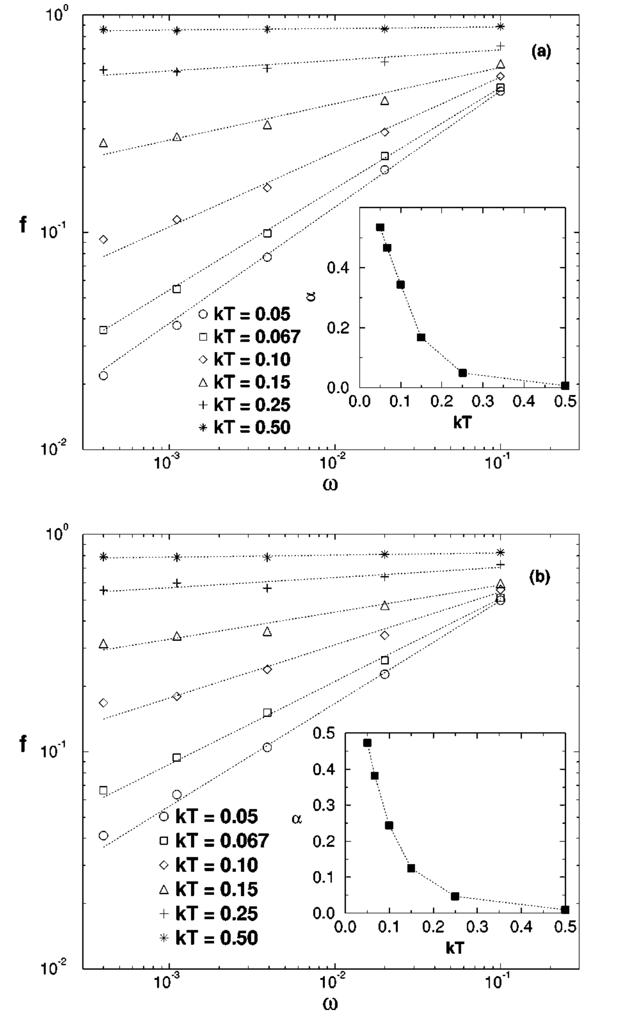

FIG. 4. Correlation factor f vs update frequency ω at different temperatures: (a) for the uniform PDF; (b) for the exponential PDF. Inlets show the variation of the respective exponent α with temperature.

As one may readily verify from Fig. 2(a) [Fig. 2(b)], Eq. (42) [Eq. (43)] practically coincides with our data points in the whole temperature interval for both uniform and exponential PDF's.

It is interesting to find out what features characterize the diffusive behavior in the low-temperature power-law regime. In Fig. 3 we show the measured effective activation energy $\langle E_a \rangle$ as a function of the tracer's thermal energy for the case of dynamic disorder $\omega = 1$. It is seen that at low temperature $\langle E_a \rangle \approx kT$, whereas at higher temperature $\langle E_a \rangle \rightarrow E_0$, with $E_0 = 0.5$ being the mean height of the barriers. Measurements of $\langle E_a \rangle$ vs kT at different frequencies ω (including $\omega = 0$) yield curves which are practically indistinguishable from those shown in Fig. 3, i.e., $\langle E_a \rangle$ depends only on temperature (and not on ω). Thus in all cases the tracer overcomes barriers of height which are comparable, on the average, with its thermal energy. In a frozen random medium the low-energy tracer follows easy paths, spending large periods of time in confinement between high barriers, which is manifested as anomalous diffusion, $\langle R(t)^2 \rangle \propto t^\gamma$ with $\gamma < 1$. After a characteristic time τ_c, the ''ridges'' between such low-barrier basins are overcome and diffusion turns to normal for times larger that τ_c. If time is measured in intervals larger than τ_c, the tracer has thus been given sufficient time to overcome successfully the ''ridges'' separating one valley of low barriers from the next, and explore *all* barrier heights with an average height of E_0.

Conversely, in the case of dynamic disorder the tracer particle at temperatures $kT \ll E_0$ is aided by a periodic replacement of the higher barriers by low ones, thus needing to overcome only those barriers whose height is comparable to its own thermal energy kT, as suggested by Fig. 3. Even in this case the random walks become more and more correlated within a limited region of low barriers as the thermal energy of the tracer diminishes, and, as Fig. 4 shows, the degree of these correlations is rapidly increased as the disorder renewal slows down.

Independent of the particular PDF of barriers we use, we observe essentially a power-law dependence of the correlation factor, f, on ω: $f \propto \omega^\alpha$ where the exponent α (and the degree of localization) quickly increases with decreasing temperature. At fixed temperature the degree of correlation

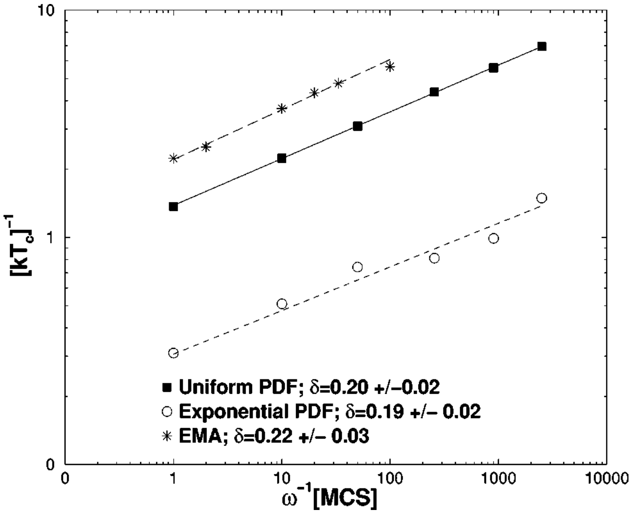

FIG. 5. Crossover temperature kT_c vs barrier update frequency ω for the uniform PDF.

in the tracer's movements decreases as ω grows, as should be expected.

The variation of the crossover temperature T_c on ω is shown on Fig. 5 to follow a power-law relationship

$$kT_c \propto \omega^{\delta}, \tag{44}$$

with $\delta = 0.21 \pm 0.02$, provided, as done in this study, one defines kT_c as the intersection point of the low-temperature tangent to D/D_0 and the Arrhenius curve exp(E/kT). Evidently, the EMA data on the scaling of T_c with ω agree reasonably well with those of the simulations, bearing in mind the low precision of such graphical T_c determination.

V. CONCLUSION

Summarizing, in the case of a RBM with *dynamic* disorder, both EMA analysis and MC simulational results for a square lattice suggest the existence of a crossover from Arrhenian to linear variation of diffusion coefficient with temperature. Following from the treatment of the model within the EMA, this happens when the probability distribution of barrier heights *includes* a zero barrier, and simulational results show that this behavior does not depend on the particular distribution function. Also the temperature of crossover kT_c scales as $kT_c \propto \omega^{0.21}$, independently of the particular probability distribution function of the barriers. For a simultaneous hop and renewal process ($\omega = 1$) a simple analytical result reproduces perfectly the observed linear relationship $D/D_0 \approx kT$.

ACKNOWLEDGMENTS

This work was partially supported by the CONICET and Fundacion Antorchas (Argentina). The European Economic Community (Project No. ITDC-240) is greatly acknowledged for providing valuable equipment. One of us (A.M.) gratefully acknowledges support by Argentinian Project No. FOMEC 307 during a visit to the University of San Luis, Argentina.

APPENDIX

In the case of a two-dimensional system the function $\phi(\xi(s))$ [see Eq. (15)], which enters into the right-hand side of the EMA equation (14), can be expressed as an explicit function of s and $\tilde{\Gamma}(s)$ by using the well known representation of $P(\mathbf{0},\xi)$ [see Eq. (5)] at $d=2$ and $\mathbf{n}=\mathbf{0}$,

$$P(\mathbf{0},\xi) = \frac{2}{\pi}\mathcal{K}(\xi). \tag{A1}$$

Here $\mathcal{K}(k)$ the complete elliptic integral of the first kind,

$$\mathcal{K}(k) = \int_0^{\pi/2} \mathrm{d}x \frac{1}{\sqrt{1-k^2\sin^2 x}}. \tag{A2}$$

Equation (A1) can be derived by using the elementary identity

$$x^{-1} = \int_0^{\infty} dt \exp(-xt) \tag{A3}$$

valid for all $x > 0$, and the integral representation of the modified Bessel function I_0,

$$I_0(z) = \frac{1}{\pi}\int_0^{\pi} dk \exp(z \cos k). \tag{A4}$$

The derivation goes for all $\xi < 1$ as follows:

$$\begin{aligned} P(\mathbf{0},\xi) &= \frac{1}{\pi^2}\int_0^{\pi} dk_1 \int_0^{\pi} dk_2 \frac{1}{1-(\xi/2)(\cos k_1 + \cos k_2)} \\ &= \int_0^{\infty} dt \exp(-t)\left[\frac{1}{\pi}\int_0^{\pi} dk \exp\left(\frac{\xi t}{2}\cos k\right)\right]^2 \\ &= \int_0^{\infty} dt \exp(-t)\left[\mathrm{I}_0\left(\frac{\xi t}{2}\right)\right]^2 = \frac{2}{\pi}\mathcal{K}(\xi). \end{aligned} \tag{A5}$$

Thus, by substituting Eq. (A1) for $P(\mathbf{0},\xi)$ in the rhs of Eq. (14) for $\phi(\xi(s))$, keeping in mind that $\xi(s)$ depends on both s and $\tilde{\Gamma}(s)$ through Eq. (7), one finally obtains an explicit form of EMA equation (14) for the Laplace transform $\tilde{\Gamma}(s)$.

[1] I. Avramov, A. Milchev and P. Argyrakis, Phys. Rev. E **47**, 2303 (1993).
[2] A. Hörner, A. Milchev, and P. Argyrakis, Phys. Rev. E **52**, 3570 (1995).
[3] P. Argyrakis, A. Milchev, V. Pereyra, and K. Kehr, Phys. Rev. E **52**, 3623 (1995).
[4] E. Arapaki, P. Argyrakis, I. Avramov, and A. Milchev, Phys. Rev. E **56**, R29 (1997).

[5] Y. Limoge and J. L. Bocquet, Phys. Rev. Lett. **65**, 60 (1990).
[6] K. Mussawisade, T. Wichmann, and K. W. Kehr, J. Phys. Condens. Matter **9**, 1181 (1997).
[7] J. Bernasconi, W. R. Schneider, and H. J. Wiesmann, Phys. Rev. B **16**, 5250 (1977).
[8] I. Avramov, A. Milchev, E. Arapaki, and P. Argyrakis, Phys. Rev. E **58**, 2788 (1998).
[9] S. D. Drugger, A. Nitzan, and M. A. Ratner, J. Chem. Phys. **79**, 3133 (1983).
[10] S. D. Drugger, M. A. Ratner, and A. Nitzan, Phys. Rev. B **31**, 3939 (1985).
[11] A. Nitzan and M. A. Ratner, J. Phys. Chem. **98**, 1765 (1994).
[12] S. Summerfield, Solid State Commun. **39**, 401 (1981).
[13] T. Odagaki and M. Lax, Phys. Rev. B **24**, 5284 (1981).
[14] I. Webman, Phys. Rev. Lett. **47**, 1496 (1981).
[15] J. W. Haus and K. W. Kehr, Phys. Rep. **150**, 263 (1987).